IMAGE DEBLURRING IN THE PRESENCE OF SALT-AND-PEPPER NOISE

Liming Hou[1], *Hongqing Liu*[1], *Zhen Luo*[1], *Yi Zhou*[2], *and Trieu-Kien Truong*[3]

[1] Chongqing Key Lab of Mobile Communications Technology,
Chongqing University of Posts and Telecommunications, Chongqing, China.
E-mail: hongqingliu@outlook.com.
[2]School of Communication and Information Engineering,
Chongqing University of Posts and Telecommunications, Chongqing, China.
[3] Department of Information Engineering, I-Shou University.

ABSTRACT

This work addresses image recovery problem in the presence of salt-and-pepper noise and image blur. The salt-and-pepper noise reviewed as the impulsive noise, in this paper, is modeled as a sparse signal because of its impulsiveness. To accurately reconstruct the clean image and the blur kernel, the framelet domains are exploited to sparsely represent the image and the blur kernel. From the reformulations conducted, a joint estimation is devised to simultaneously perform the image recovery, the salt-and-pepper noise suppression and the blur kernel estimation under a optimization framework. To solve the optimization problem, an efficient solver based on accelerated proximal gradient (APG) is developed to obtain the joint estimation solution. Numerical studies demonstrate the superior performance of the joint estimation algorithm compared with the state-of-the-art approaches in terms of both objective and subjective evaluation standards.

Index Terms— Image recovery, salt-and-pepper noise, blur kernel, sparsity, joint estimation.

1. INTRODUCTION

Image restoration is a fundamental and widely studied subject in image processing where the main purpose is to reconstruct the clean image from the degraded and/or noisy image [1–3]. In this work, the image restoration problem is studied in the presence of salt-and-pepper noise and image blur.

The combination of the salt-and-pepper noise and blurring brings a great challenge to perform image reconstruction. The classical methods developed for Gaussian noise produces very poor results. To benefit from the fact that parts of the pixels are noise-free, a two-phase method that includes first noise detection and then deblur based on the noise-free pixels was proposed in [4], and after that two improved versions based on the similar idea were developed in [5] and [6]. They all use a noise detector to distinguish pixels which are likely to be corrupted by noise in the first phase and then estimate the clear image by using the available information on noise-free pixels detected. Unfortunately, there are two unavoidable issues. First, the blurring kernel is assumed to be known while it is not the case in practice. Second, there is a rapid descend in performance when the noise level is high because of the limited noise-free pixels.

To increase the practical usages dealing with salt-and-pepper noise and blurring, in this paper, a joint estimation approach is designed to simultaneously recover the image and blurring kernel in the presence of the salt-and-pepper noise, demonstrated in Figure 1. To achieve so, the sparse domains are utilized where the unknown kernel and image have sparse representations in framelet domain, and noise is sparsely represented by spatial domain. Therefore, based on the sparse properties, the joint optimization is developed in terms of unknown kernel, image, and noise. To efficiently solve this optimization problem, a two-step iterative approach is proposed where each step contains a ℓ_1-norm optimization problem, and accelerated proximal gradient (APG) is tailored to solve the optimization problems. Numerical experiments demonstrate that the proposed approach is a promising candidate in recovering image in the presence of the salt-and-pepper noise and image blur.

2. FORMULATIONS OF SALT-AND-PEPPER NOISE

The objective of a common image reconstruction is to recover the clean image from the degraded and/or noisy image, which is a classical inverse problem, given by

$$\mathbf{y} = \mathbf{H}\mathbf{x} + \mathbf{n}, \tag{1}$$

where $\mathbf{y}$ is the observed image, $\mathbf{x}$ is the clean image to be recovered, $\mathbf{H}$ is the degradation matrix, and $\mathbf{n}$ is the noise.

This work was jointly supported by the National Natural Science Foundation of China under Grant 61501072, by Foundation and Advanced research projects of Chongqing Municipal Science and Technology Commission under Grant cstc2015jcyjA40027, by the Ministry of Education Scientific Research Foundation for Returned Overseas Chinese F201405.

(a) The original image

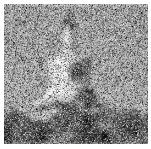

(b) The noisy blurred image

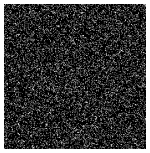

(c) Our reconstructed results

Fig. 1: The reconstructed image, blurring kernel, and salt-and-pepper noise by proposed method.

Note that the column representation of the image is utilized in (1).

For the problems studied in this work, the degradation matrix is an blur operator and the noise $\mathbf{n}$ is the salt-and-pepper noise that is one type of impulsive noises. Suppose the clean image is corrupted by the salt-and-pepper noise, and the noisy pixel is

$$y(i) = \begin{cases} n_{min}, & \text{with probability } p/2 \\ n_{max}, & \text{with probability } p/2 \\ x(i), & \text{with probability } 1-p \end{cases} \tag{2}$$

where p denotes the noise level, n_{min} and n_{max} represent the minimum and maximum values of the image dynamic range, for example, they are 0 and 255 for a grey image, respectively. One important character of the noise model in (2) is that only $p \times 100\%$ pixels are affected by the noise and the rest is not. From this observation and if the additive noise model in (1) is utilized, the noise $\mathbf{n}$ contains lots of zero components. This implies that $\mathbf{n}$ can be viewed as a sparse vector and this property will be explored to remove the noise [7].

The objective of this work is to simultaneously perform the deblur and image recovery in the presence of the salt-and-pepper noise, by utilizing the sparse properties of the signals.

3. PROBLEM FORMULATION AND ALGORITHM DEVELOPMENT

It is well-known that an image has a sparse structure in different transform domains, for example, wavelet, framelet, to name a few. To reveal the sparse structure of the image and blur kernel, the framelet domain is utilized in this work. Due to the space limitation, the description of the framelet is omitted, the interested readers are referred to [8]. We use $\mathcal{W}$ to represent the tensor product framelet decomposition and $\mathcal{W}^{\mathrm{T}}$ to denote the framelet reconstruction, and therefore, the degraded image in (1) is rewritten as

$$\mathbf{y} = (\mathcal{W}^{\mathrm{T}}\boldsymbol{\alpha}_H)(\mathcal{W}^{\mathrm{T}}\boldsymbol{\alpha}_x) + \mathbf{n}, \tag{3}$$

where $\boldsymbol{\alpha}_H$ is the framelet coefficient vector for blur kernel that is unknown and sparse, and $\boldsymbol{\alpha}_x$ is the framelet coefficient vector for image that is also unknown and sparse. In the deblur process, it is found that the results are very sensitive to the error in blur kernel. To perform the recovery in a robust manner, the following model is developed for image deblur

$$\begin{aligned} \mathbf{y} &= (\mathcal{W}^{\mathrm{T}}\boldsymbol{\alpha}_H + \delta)(\mathcal{W}^{\mathrm{T}}\boldsymbol{\alpha}_x) + \mathbf{n}, \\ &= (\mathcal{W}^{\mathrm{T}}\boldsymbol{\alpha}_H)(\mathcal{W}^{\mathrm{T}}\boldsymbol{\alpha}_x) + \mathbf{u} + \mathbf{n}, \end{aligned} \tag{4}$$

where $\mathbf{u} = \delta(\mathcal{W}^{\mathrm{T}}\boldsymbol{\alpha}_x)$ is the residual term, and it has been shown to be sparse in the spatial domain [9]. To explore the sparse property of the $\boldsymbol{\alpha}_x$, $\boldsymbol{\alpha}_h$, $\mathbf{u}$ and $\mathbf{n}$, the following optimization problem is proposed to jointly perform image reconstruction and blurring kernel estimation under the salt-and-pepper noise. That is

$$\begin{aligned} &\text{minimize} \;\; \|\boldsymbol{\alpha}_x\|_1 + \lambda_1\|\boldsymbol{\alpha}_H\|_1 + \lambda_2\|\mathbf{n}\|_1 + \lambda_3\|\mathbf{u}\|_1 \\ &\text{subject to} \;\; \|\mathbf{y} - (\mathcal{W}^{\mathrm{T}}\boldsymbol{\alpha}_H)(\mathcal{W}^{\mathrm{T}}\boldsymbol{\alpha}_x) - \mathbf{u} - \mathbf{n}\|_2^2 < \epsilon, \end{aligned} \tag{5}$$

with variables $\boldsymbol{\alpha}_x$, $\boldsymbol{\alpha}_H$, $\mathbf{u}$ and $\mathbf{n}$. To efficiently solve the optimization problem in (4), a two-step iterative process is utilized. First, suppose $\boldsymbol{\alpha}_H$ and $\mathbf{u}$ are known, the sub-problem becomes a convex optimization problem with variables $\boldsymbol{\alpha}_x$ and $\mathbf{n}$, and then it can be efficiently solved. Second, with the estimated $\boldsymbol{\alpha}_x$ and $\mathbf{n}$, the sub-problem also is a convex optimization with variables $\boldsymbol{\alpha}_H$ and $\mathbf{u}$. In details, the two-step procedure works as follows.

Initialize the blurring kernel.

• **Step 1***: solve the convex optimization problem of* (5) *with the initialized/estimated blurring kernel to produce estimations of* $\boldsymbol{\alpha}_x$ *and* $\mathbf{n}$ *as*

$$\begin{aligned} &\text{minimize} \;\; \|\boldsymbol{\alpha}_x\|_1 + \lambda_2\|\mathbf{n}\|_1 \\ &\text{subject to} \;\; \|\mathbf{y} - (\mathcal{W}^{\mathrm{T}}\hat{\boldsymbol{\alpha}}_H)(\mathcal{W}^{\mathrm{T}}\boldsymbol{\alpha}_x) - \hat{\mathbf{u}} - \mathbf{n}\|_2 < \epsilon, \end{aligned} \tag{6}$$

where $\hat{\alpha}_H$ *and* $\hat{\mathbf{u}}$ *indicates the initialized/estimated value of the kernel and residual term respectively.*

• **Step 2***: Using the estimations from Step 1, solving the same convex optimization problem of* (5) *produces blurring kernel estimation as*

$$\begin{aligned} &\text{minimize} \;\; \|\boldsymbol{\alpha}_H\|_1 + \lambda_2\|\mathbf{u}\|_1 \\ &\text{subject to} \;\; \|\mathbf{y} - (\mathcal{W}^{\mathrm{T}}\boldsymbol{\alpha}_H)(\mathcal{W}^{\mathrm{T}}\hat{\boldsymbol{\alpha}}_x) - \mathbf{u} - \hat{\mathbf{n}}\|_2 < \epsilon, \end{aligned} \tag{7}$$

where $\hat{\boldsymbol{\alpha}}_x$ *and* $\hat{\mathbf{n}}$ *represent the estimated values of* $\boldsymbol{\alpha}_x$ *and* $\mathbf{n}$*, respectively.*

• *Steps 1 and 2 are proceeded recursively until a stopping rule is satisfied.*

Table 1: Algorithm 1: APG based approach.

Objective function: $\lambda_1\|\boldsymbol{\alpha}_x|_1+\lambda_2\|\boldsymbol{\alpha}_H|_1+\lambda_3\|\mathbf{n}\|_1+\lambda_4\|\mathbf{u}\|_1+\|\mathbf{y}-(\mathcal{W}^{\mathrm{T}}\boldsymbol{\alpha}_H)(\mathcal{W}^{\mathrm{T}}\boldsymbol{\alpha}_x)-\mathbf{u}-\mathbf{n}\|_2^2$
Outputs: Estimates of $\mathbf{n}$, $\boldsymbol{\alpha}_x$ and $\boldsymbol{\alpha}_H$

Initialization: $l=0$, $\mathbf{n}_0=\mathbf{n}_{-1}$, $\boldsymbol{\alpha}_{x,0}=\boldsymbol{\alpha}_{x,-1}$, $\boldsymbol{\alpha}_{H,0}=\boldsymbol{\alpha}_{H,-1}$, $\mathbf{u}_0=\mathbf{u}_{-1}$, $t_0=1, t_{-1}=0$
Repeat
$\beta_l^{\mathbf{n}}=\mathbf{n}_l+\frac{t_{l-1}}{t_l}(\mathbf{n}_l-\mathbf{n}_{l-1})$
$\beta_l^{\boldsymbol{\alpha}_x}=(\boldsymbol{\alpha}_{x,l}+\frac{t_{l-1}}{t_l}(\boldsymbol{\alpha}_{x,l}-\boldsymbol{\alpha}_{x,l-1})$
$\beta_l^{\boldsymbol{\alpha}_H}=\boldsymbol{\alpha}_{H,l}+\frac{t_{l-1}}{t_l}(\boldsymbol{\alpha}_{H,l}-\boldsymbol{\alpha}_{H,l-1})$
$\beta_l^{\mathbf{u}}=\mathbf{u}_l+\frac{t_{l-1}}{t_l}(\mathbf{u}_l-\mathbf{u}_{l-1})$
$\mathbf{n}_{l+1}=\mathbf{T}_{\lambda_1/L}(\beta_l^{\mathbf{n}}-\nabla_{\mathbf{n}}F(\beta_l^{\mathbf{n}},\beta_l^{\boldsymbol{\alpha}_x},\beta_l^{\boldsymbol{\alpha}_H},\beta_l^{\mathbf{u}})/L)$
$\boldsymbol{\alpha}_{x,l+1}=\mathbf{T}_{\lambda_2/L}(\beta_l^{\boldsymbol{\alpha}_x}-\nabla_{\boldsymbol{\alpha}_x}F(\beta_l^{\mathbf{n}},\beta_l^{\boldsymbol{\alpha}_x},\beta_l^{\boldsymbol{\alpha}_H},\beta_l^{\mathbf{u}})/L)$
$\boldsymbol{\alpha}_{H,l+1}=\mathbf{T}_{\lambda_3/L}(\beta_l^{\boldsymbol{\alpha}_H}-\nabla_{\boldsymbol{\alpha}_H}F(\beta_l^{\mathbf{n}},\beta_l^{\boldsymbol{\alpha}_x},\beta_l^{\boldsymbol{\alpha}_H},\beta_l^{\mathbf{u}})/L)$
$\mathbf{u}_{l+1}=\mathbf{T}_{\lambda_4/L}(\beta_l^{\mathbf{u}}-\nabla_{\mathbf{u}}F(\beta_l^{\mathbf{n}},\beta_l^{\boldsymbol{\alpha}_x},\beta_l^{\boldsymbol{\alpha}_H},\beta_l^{\mathbf{u}})/L)$
$t_{l+1}=\frac{1+\sqrt{1+4t_l^2}}{2}$
$l=l+1$
Until $l>T$ {maximum iteration} or $\|\mathcal{W}^{\mathrm{T}}(\boldsymbol{\alpha}_{x,l+1}-\boldsymbol{\alpha}_{x,l})\|_2<\delta$ {predefined threshold}.

At each step of the two-step process, it solves an ℓ_1-norm constrained optimization problem, and considering the large size of the image, the algorithm of APG is tailored to solve the optimization problem and it is summarized in Table 1, where the $\mathbf{T}(\cdot)$ represents the soft thresholding operation.
To implement the APG algorithm in Table 1, the gradients of data fidelity function in terms of optimization variables are required, and they respectively are

$$\begin{aligned}
&\nabla_{\mathbf{n}}F=-2(\mathbf{y}-(\mathcal{W}^{\mathrm{T}}\boldsymbol{\alpha}_H)(\mathcal{W}^{\mathrm{T}}\boldsymbol{\alpha}_x)-\mathbf{u}-\mathbf{n}),\\
&\nabla_{\boldsymbol{\alpha}_x}F=-2\mathcal{W}(\mathcal{W}^{\mathrm{T}}\boldsymbol{\alpha}_x)^{\mathrm{T}}(\mathbf{y}-(\mathcal{W}^{\mathrm{T}}\boldsymbol{\alpha}_H)(\mathcal{W}^{\mathrm{T}}\boldsymbol{\alpha}_x)-\mathbf{u}-\mathbf{n}),\\
&\nabla_{\boldsymbol{\alpha}_H}F=-2\mathcal{W}(\mathcal{W}^{\mathrm{T}}\boldsymbol{\alpha}_H)^{\mathrm{T}}(\mathbf{y}-(\mathcal{W}^{\mathrm{T}}\boldsymbol{\alpha}_H)(\mathcal{W}^{\mathrm{T}}\boldsymbol{\alpha}_x)-\mathbf{u}-\mathbf{n}),\\
&\nabla_{\mathbf{u}}F=-2(\mathbf{y}-(\mathcal{W}^{\mathrm{T}}\boldsymbol{\alpha}_H)(\mathcal{W}^{\mathrm{T}}\boldsymbol{\alpha}_x)-\mathbf{u}-\mathbf{n}),
\end{aligned}\tag{8}$$

where

$$F(\mathbf{n},\boldsymbol{\alpha}_x,\boldsymbol{\alpha}_H,\mathbf{u})=\|\mathbf{y}-(\mathcal{W}^{\mathrm{T}}\boldsymbol{\alpha}_H)(\mathcal{W}^{\mathrm{T}}\boldsymbol{\alpha}_x)-\mathbf{u}-\mathbf{n}\|_2^2$$

4. NUMERICAL STUDIES

The results of numerical studies are presented in this section to demonstrate the performance of the proposed joint estimation method. For comparison purpose, the results from TP-TV [5], and FTP [6] are also provided, and the parameters of them are set to be the best. In APG, the parameters of λ, L and T for the estimation of $\boldsymbol{\alpha}_x$, $\mathbf{n}$, $\boldsymbol{\alpha}_H$ and $\mathbf{u}$ are chosen as 0.0002, 2, 600, 0.002, 2, 600, 0.003, 3, 30 and 0.0005, 3, 30 respectively. In our experiments, we consider three different blurring operators, which are Gaussian blur with a window size of 9×9 and a standard deviation of 5, out-of-focus blur with radius 5, and motion blur with length 20 and angle 20. The restoration performances are quantitatively measured by the peak signal-to-noise ratio (PSNR).

First and foremost, in Figure 1, we would like to showcase the ability of the proposed method that can simultaneously estimate image, blur kernel and the noise, where the recontracted image, blur kernel and noise match original ones well. In the first case of the experiments, we fix the blur kernel that is Gaussian one, and the restored images of *house* are provided in Figure 2 under the cases of different levels of noise. It is seen that when the noise level increases, the performance of all the approaches degrades, but the proposed method outperforms others by producing the highest PSNRs in all cases. In the second case, the noise level is fixed that is 50%, and the restored images of *house* are provided in Figure 3 for different blur kernels. The ringing artifacts are noticeable in the results obtained by the FTP, whereas the proposed approach preserves the details of the image. In Table 2, the PSNRs are provided under the cases of different blurs and noise levels, and it is seen that the proposed method produces the best PSNRs for all scenarios.

5. CONCLUSION

In this work, the image and the kernel are sparsely represented by the framelet domain, and the noise is sparsely represented by the spatial domain. To perform robust recovery, the estimation error in blur kernel is also considered and sparely represented by spatial domain. Based on the sparse properties, a joint estimation is devised that simultaneously recovers the image, suppresses the noise, and estimates the unknown blurring kernel. A two-step process is developed to obtain the solution in which the APG approach is applied to efficiently solve ℓ_1-norm constrained problem. Numerical studies demonstrate that the proposed proposed joint estimation approach offers great performance improvements compared with other state-of-the-art algorithms.

image	p× 100%	Gaussian			motion			out-of-focus		
		TP-TV	FTP	Our	TP-TV	FTP	Our	TP-TV	FTP	Our
house	30%	34.82	34.70	**37.80**	34.10	34.71	**35.12**	35.56	35.08	**37.73**
	50%	34.27	33.75	**36.59**	33.17	33.16	**33.49**	34.72	33.75	**35.63**
	70%	33.04	32.27	**34.25**	31.27	30.69	**31.36**	33.13	31.92	**33.19**
lena	50%	29.02	28.75	**29.14**	29.91	29.33	**30.11**	30.48	29.87	**30.65**
barbara		26.59	27.21	**28.58**	25.90	26.86	**27.02**	26.99	27.61	**28.61**
cameraman		27.46	26.72	**27.56**	27.63	26.81	**28.13**	28.49	27.23	**28.57**

Table 2: PSNRs(dB) for recovered images of different blurs and levels of salt-and-pepper noise.

Fig. 2: The noisy blurred image (fist row, Gaussian blur), TP-TV (second row), FTP (third row) and proposed method (fourth row) with different levels of salt-and-pepper noise: $p = 0.2$ (first column), $p = 0.4$ (second column), $p = 0.6$ (third column).

Fig. 3: The noisy blurred image (fist row, $p = 0.5$), TP-TV (second row), FTP (third row) and proposed method (fourth row) with different blur operators: Gaussian blur (first column), motion blur (second column), and out-of-focus blur (third column).

6. REFERENCES

[1] M. Elad and M. Aharon, "Image denoising via sparse and redundant representations over learned dictionaries," *IEEE Trans. Image Process.*, vol. 15, no. 12, pp. 3736–3745, Dec. 2006.

[2] A. Beck and M. Teboulle, "Fast gradient-based algorithms for constrained total variation image denoising and deblurring problems," *IEEE Trans. Image Process.*, vol. 18, no. 11, pp. 2419–2434, Nov. 2009.

[3] M. Zhou, H. Chen, J. Paisley, L. Ren, L. Li, Z. Xing, D. Dunson, G. Sapiro, and L. Carin, "Nonparametric bayesian dictionary learning for analysis of noisy and incomplete images," *IEEE Trans. Image Process.*, vol. 21, no. 1, pp. 130–144, Jan. 2012.

[4] J. F. Cai, R. H. Chan, and M. Nikolova, "Two-phase approach for deblurring images corrupted by impulse plus gaussian noise," *Inverse Problems*, vol. 18, no. 2, pp. 187–204, 2008.

[5] J. F. Cai, R. H. Chan, and M. Nikolova, "Fast two-phase image deblurring under impulse noise," *Journal of Mathematical Imaging*, vol. 8, no. 36, pp. 46–253, 2010.

[6] R. H. Chan, Y. Dong, and M. Hintermuller, "An efficient two-phase ℓ_1-TV method for restoring blurred images with impulse noise," *IEEE Trans. Image Process.*, vol. 9, no. 7, pp. 1731–1739, Jul. 2010.

[7] H.Q.Liu, Y. Li, Y. Zhou, H.-C. Chang, and T.-K. Truong, "Impulsive noise suppression in the case of frequency estimation by exploring signal sparsity," *Digital Signal Processing*, vol. 57, pp. 34–45, Oct. 2016.

[8] I. Daubechies, B. Han, A. Ron, and Z. Shen, "Framelets: MRA-based constructions of wavelet frames," *Appl. Comput. Harmon. Anal.*, vol. 14, pp. 1–46, 2003.

[9] H. J and K. Wang, "Robust image deblurring with an inaccurate blur kernel," *IEEE Trans. Image Process.*, vol. 21, no. 11, pp. 1624–1634, 2012.